

Demethylation of *HACE1* gene promoter by propofol promotes autophagy of human A549 cells

SHANSHAN LI, HUI YANG, MIN ZHAO, LINLI GONG, YAHONG WANG,
ZHIYONG LV, YUHANG QUAN and ZHONGHUI WANG

Department of Anesthesiology, The Third Affiliated Hospital of Kunming Medical University
(Tumor Hospital of Yunnan Province), Kunming, Yunnan 650118, P.R. China

Received February 13, 2020; Accepted August 28, 2020

DOI: 10.3892/ol.2020.12143

Abstract. Propofol (2,6-diisopropylphenol) is one of the most commonly used intravenous anesthetics and possesses a number of non-anesthetic effects, including antitumor function. The aim of the present study was to elucidate the antitumor molecular mechanism of propofol on A549 and H1299 cells. A549 and H1299 cells were treated in the presence or absence of different concentrations (0, 60 or 120 μ mol) of propofol for different durations (0, 24, 48 or 72 h), and proliferation was detected by MTT and colony formation assays; the protein levels of optineurin (OPTN) ubiquitination, HECT domain and ankyrin repeat containing E3 ubiquitin protein ligase 1 (*HACE1*), methyl-CpG binding domain protein 3 (MBD3) and Microtubule-associated protein 1A/1B-light chain 3 were detected by immunoblotting or quantitative (q)PCR; the methylation state of the *HACE1* gene promoter was detected by bisulfite DNA sequencing; and binding of MBD3 on *HACE1* gene promoter was detected by chromatin immunoprecipitation-qPCR. Propofol inhibited proliferation of A549 and H1299 cells and promoted *HACE1*-OPTN axis-mediated selective autophagy activity by increasing the protein expression levels of *HACE1* via demethylating its promoter region. Furthermore, propofol promoted expression levels of MBD3 and binding to the -1,000 to -1 bp (transcription start site) region of *HACE1* gene promoter. MBD3-knockdown experiments indicated that propofol inhibited proliferation of A549 cells in a MBD3-dependent manner. Thus, the findings of the present study provided a potential antitumor molecular mechanism mediated by propofol.

Introduction

Anesthetics are important chemical drugs that allow patients to undergo operations involving severe pain where the patient must not move, such as dental treatment (1,2). Propofol (2,6-diisopropylphenol) is one of the most commonly used intravenous anesthetics globally as the depth of anesthesia induced by propofol can be controlled to a greater degree compared with other anesthetics, such as midazolam, etomidate, thiopental sodium and ketamine (1,3-5). At the same time, propofol possesses a number of non-anesthetic effects, including antitumor function, which has been widely reported (6,7).

Lung cancer is a leading cause of mortality worldwide and accounts for >1,000,000 deaths every year (6,8,9). The 5-year survival rate of patients with lung cancer is <17% (6). Different anticancer strategies have been developed and used in clinical treatment of lung cancer, including surgery, chemotherapy, immunotherapy and targeted therapy (10-13). However, these strategies do not effectively improve the long-term survival rate of patients with lung cancer, so novel effective therapeutic interventions and targets are urgently needed. Propofol suppresses growth, migration and invasion of human lung adenocarcinoma A549 cells by upregulation of microRNA (miR)-1284 and downregulation of miR-372 (6,14). Considering propofol is widely used in clinical practice, it is important to explore the association between propofol and lung cancer, as well as the underlying molecular mechanisms.

Autophagy is a conserved complex process which maintains the normal function and structure of cells (15,16). Autophagy is involved in the occurrence and progression of lung cancer. For example, Xue *et al* (17) demonstrated that apoptosis stimulating protein of p53 promotes tumor growth by increasing autophagic flux in human non-small cell lung cancer, whereas HECT domain and ankyrin repeat containing E3 ubiquitin protein ligase 1 (*HACE1*) acts as a tumor suppressor by ubiquitinating optineurin (OPTN) and activating selective autophagy (18). Autophagy is also involved in lung cancer therapy, chemotherapy induces tumor cell autophagy, and inhibiting autophagy enhances the sensitivity of lung cancer cells to chemotherapy (19).

The association between propofol and autophagy is complex. For example, propofol attenuates hypoxia/reoxygenation-induced

Correspondence to: Professor Zhonghui Wang, Department of Anesthesiology, The Third Affiliated Hospital of Kunming Medical University (Tumor Hospital of Yunnan Province), 519 Kunzhou Road, Kunming, Yunnan 650118, P.R. China
E-mail: fengliya@163.com

Key words: propofol, HECT domain and ankyrin repeat containing E3 ubiquitin protein ligase 1, demethylation, autophagy, methyl-CpG binding domain protein 3

autophagy in HK-2 cells, but induces autophagy in C2C12 cells (16). The present study aimed to elucidate the antitumor molecular mechanism of propofol on human lung adenocarcinoma cells and its potential application on lung cancer therapy.

Materials and methods

Plasmid construction. Short hairpin (sh)RNAs for *MBD3* and *HACE1* were designed and inserted into pLKO.1 plasmid purchased from Sigma-Aldrich (Merck KGaA); their specific sequences are provided in Table I.

Cell culture and transfection. Human A549 and H1299 cell lines were purchased from American Type Culture Collection and cultured in DMEM (Thermo Fisher Scientific, Inc.) supplemented with 10% FBS, 100 U/ml penicillin and 100 mg/ml streptomycin (all Gibco; Thermo Fisher Scientific, Inc.) in a 37°C humidified atmosphere of 5% CO₂. The plasmids containing *MBD3* or *HACE1* shRNA (3 µg) were transfected into A549 cells using Lipofectamine® 2000 (Thermo Fisher Scientific, Inc.) according to the manufacturer's instructions, and screened using puromycin (5 µg/ml, Thermo Fisher Scientific, Inc.) for 48 h after transfection.

Propofol and cycloheximide (CHX) treatment. Pure propofol was purchased from Sigma-Aldrich (Merck KGaA) and stock solution of propofol (21 mmol/l) was prepared in DMSO (Sigma-Aldrich; Merck KGaA). The propofol concentrations used were as previously described (20). The stock solution of propofol was diluted to 0.21, 0.18, 0.15, 0.12, 0.09, 0.06 and 0.03 mmol/l with DMSO (<1%) before addition to DMEM medium supplemented with 10% FBS, 100 U/ml penicillin and 100 mg/ml streptomycin (1:100). A549 and H1299 cells treated with the indicated concentrations of propofol were diluted from stock solution and an equal volume of DMSO was added to the controls (A549 or H1299 cells that did not receive propofol treatment). CHX was purchased from Sigma-Aldrich (Merck KGaA), and stock solution of CHX (100 µg/ml) was prepared in DMSO. For protein stability experiments, A549 cells were treated with CHX (100 µg/ml) as well as propofol at the indicated time point (0, 2 or 4 h) at 37°C.

Cell proliferation assay. A total of 3,000 cells was seeded into 96-well plates and treated in the presence or absence of propofol. The 0 h time point was defined as 6 h after cells were seeded. After 0, 24, 48 or 72 h, the cells were incubated with MTT solution (cat. no. C0009; Beyotime Institute of Biotechnology) for 4 h at 37°C, then the product (formazan) was dissolved in DMSO and quantified spectrophotometrically at a wavelength of 570 nm using a Microplate Reader (Bio-Rad Laboratories, Inc.). Experiments were conducted with six replicates and repeated three times.

Colony formation assay. A total of 1,000 cells was seeded into 6-well plates and treated in the presence or absence of propofol. After 7 days, plates were fixed with 4% paraformaldehyde (Merck KGaA) at room temperature for 30 min, stained with 0.1% crystal violet (cat. no. C0121; Beyotime Institute of Biotechnology) at room temperature for 30 min and washed three times with PBS buffer. Images were captured using a

Table I. Sequences of shRNAs for *MBD3* and *HACE1*.

shRNA	Target site sequence (5'→3')
<i>MBD3</i>	
Scramble	GCGCGATAGCGCTAATAATTT
shMBD3-1	AGCAACAAGGTCAAGAGCGAC
shMBD3-2	GACCTGAGCACCTTCGACTTC
shMBD3-3	GCCGGTGACCAAGATTACCAA
<i>HACE1</i>	
shHACE1-1	CCAGAAATTGATGTGAGTGAT
shHACE1-2	GCTGTGCCATATACTCCAAAT

shRNA, short hairpin RNA; *MBD3*, methyl-CpG binding domain protein 3; *HACE1*, HECT domain and ankyrin repeat containing E3 ubiquitin protein ligase 1.

camera, the number of colonies were counted manually and the average number were calculated.

Reverse transcription-quantitative (RT-q) PCR. Total RNA was extracted from cells using a total RNA kit (Tiangen Biotech Co., Ltd.). Complementary DNA was synthesized using ReverTra Ace qPCR RT Master Mix (Toyobo Life Science) at 37°C for 15 min, and 95°C for 5 min, according to the manufacturer's protocol. RT-qPCR was performed on an ABI 7500 fast real-time PCR system (pre-denaturation at 95°C for 2 min; denaturation at 95°C for 30 sec, annealing/extension at 60°C for 34 sec, 40 cycles; Applied Biosystems; Thermo Fisher Scientific, Inc.) to assess the relative abundance of *HACE1* and *MBD3* mRNA using specific primers (Table II) with staining by SYBR Green (Toyobo Life Science). The relative abundance of *HACE1* and *MBD3* was normalized to that of *GAPDH* using the 2^{-ΔΔC_q} method (21,22). A total of three independent experiments was performed.

Bisulfite DNA sequencing. Genomic DNA (gDNA) was extracted from A549 cells treated in the presence or absence of propofol using the standard phenol-chloroform extraction method (23). Then, gDNA was treated with bisulfite using the CpGenome Turbo Bisulfite Modification kit (EMD Millipore) according to the manufacturer's instructions (24). The modified DNA was amplified using Platinum Taq DNA Polymerase (Thermo Fisher Scientific, Inc.) with the respective primer sets (Table II) that recognize bisulfite-modified DNA only. Then, PCR products were cloned into the pMD18-T vector (Takara Bio, Inc.) and Sanger sequencing was performed by an external company (BioSune Bio, Inc; www.biosune.com).

Immunoprecipitation and immunoblotting. For immunoprecipitation, cells were lysed in RIPA buffer [50 mM Tris-HCl (pH 7.6), 150 mM NaCl, 5 mM EDTA, 0.1% SDS and 1% NP-40] supplemented with a protease inhibitor cocktail, cell lysates were centrifuged at 4°C with 12,000 x g for 10 min, incubated with OPTN antibody (1:100; cat. no. 10837-1-AP; ProteinTech Group, Inc.) or normal rabbit IgG (1:100; cat. no. 2729; Cell Signaling Technology, Inc.), and Protein G agarose beads (Merck KGaA) overnight at 4°C, washed three

Table II. Sequences of primers used for RT-qPCR, ChIP-qPCR and bisulfite DNA sequencing.

A, RT-qPCR		
Target gene	Forward primer (5'→3')	Reverse primer (5'→3')
<i>GAPDH</i>	AGGTGAAGGTCGGAGTCAACG	CTCAGCCTTGACGGTGCCAT
<i>HACE1</i>	TGCCAGAACGGTCACAAGACG	CTGTGCTGTATCTCTTGACCATGA
<i>Methyl-CpG binding domain protein 3</i>	GAGAGGGAAGAAGTGCCCAGAAG	GGAAGTCGAAGGTGCTCAGGTC
B, ChIP-qPCR		
Target gene	Forward primer (5'→3')	Reverse primer (5'→3')
F1R1	TTTGCTTCCCACCCATTTTCCTG	CTTCTGTGGCCCAGACAGTTTCAAC
F2R2	AAGAGGCCAAGCAAGACTGGAAC	CATTGCACTCCAGCCTGGGT
F3R3	AAGTGTTCAACTTCTGTGCAGAGC	GACACAGCCTAGTGGGAAATCCA
C, Bisulfite DNA sequencing		
Target gene	Forward primer (5'→3')	Reverse primer (5'→3')
<i>HACE1</i> promoter	ATAGGGATATAATATAGTTTAA	AAAAACTATAATTTCCAACATA

RT-q, reverse transcription-quantitative; ChIP, chromatin immunoprecipitation; *HACE1*, HECT domain and ankyrin repeat containing E3 ubiquitin protein ligase 1. F, forward primer; R, reverse primer.

times with COIP buffer at 4°C. The immunoprecipitates were enriched and denatured at 100°C for 10 min in 2X SDS-PAGE loading buffer. The inputs, immunoprecipitates and cell lysates (10 µl/lane) were then subjected to SDS-PAGE (10%) and transferred to PVDF membranes (Bio-Rad Laboratories, Inc.) with 200 mA for three hours as previously described (25). The membrane was blocked with 5% non-fat milk at room temperature for 1 h and incubated with appropriate antibodies against GAPDH (1:5,000; cat. no. 60004-1-Ig; ProteinTech Group, Inc.), *HACE1* (1:1,000; cat. no. ab133637; Abcam), ubiquitin (1:500; cat. no. sc-47721; Santa Cruz Biotechnology, Inc.), OPTN (1:2,000), microtubule-associated protein 1A/1B-light chain 3 (LC3) (1:500; cat. no. L7543; Sigma-Aldrich; Merck KGaA), MBD3 (1:1,000; cat. no. 14258-1-AP; ProteinTech Group, Inc.), tet methylcytosine dioxygenase (TET)1 (1:1,000; cat. no. 61444; Active Motif, Inc.), TET2 (1:1,000; cat. no. 21207-1-AP; ProteinTech Group, Inc.), metastasis-associated 1 family member 2 (MTA2) (1:1,000; cat. no. 66195-1-Ig; ProteinTech Group, Inc.) or TET3 (1:800; cat. no. 61395; Active Motif, Inc.) overnight at 4°C, washed three times with TBST (50 mM Tris-HCl, 150 mM NaCl and 0.1% Tween-20, pH 7.6), and then incubated with secondary antibodies [HRP-conjugated Affinipure Goat Anti-Mouse IgG (H+L), cat. no. SA00001-1, 1:5,000 dilution; HRP-conjugated Affinipure Goat Anti-Rabbit IgG (H+L), cat. no. SA00001-2, 1:5,000 dilution.] at room temperature for one hour, washed three times with TBST, the signals were visualized with high-sig ECL Western Blotting Substrate (cat. no. 180-5001, Tanon Science and Technology Co., Ltd.) using a Tanon 5200 Imaging System (Tanon Science and Technology Co., Ltd.). Gray values of protein bands were quantified using ImageJ

software (version 1.52; National Institutes of Health) and calculated.

Chromatin immunoprecipitation (ChIP). ChIP experiments were performed as previously described (26). Briefly, A549 cells treated in the presence or absence of propofol were crosslinked in 1% formaldehyde (Sigma-Aldrich; Merck KGaA) for 10 min at room temperature, followed by quenching in 125 mM glycine, then washed three times with ice-cold PBS, and resuspended with 270 µl lysis buffer [50 mM Tris-Cl (pH 8.0), 10 mM EDTA, 1% SDS and protease inhibitor]. Following incubation on ice for 5 min, cells were sonicated with Bioruptor (Diagenode SA) for 15 cycles of 30 sec on, 30 sec off at high setting. Samples were centrifuged at 13,000 x g for 10 min at 4°C. Then, 100 µl supernatant was diluted 10 times with ChIP dilution buffer [20.00 mM Tris-Cl (pH 8.0), 0.01% SDS, 1.10% Triton X-100, 1.10 mM EDTA and 167.00 mM NaCl] and incubated with 5 µg control rabbit IgG (cat. no. 2729; Cell Signaling Technology, Inc.) or anti-MBD3 (cat. no. 14258-1-AP; ProteinTech Group, Inc.) antibody at 4°C overnight. Samples were further incubated with 40 µl Protein G beads at 4°C for 2 h. The beads were washed three times with low salt wash buffer [20.0 mM Tris-Cl (pH 8.0), 150.0 mM NaCl, 0.1% SDS, 1.0% Triton X-100, 2.0 mM EDTA], three times with high salt wash buffer [20.0 mM Tris-Cl (pH 8.0), 500.0 mM NaCl, 1.0% NP-40, 0.1% SDS, 2.0 mM EDTA], three times with LiCl wash buffer [20 mM Tris-Cl (pH 8.0), 500 mM LiCl, 1% NP-40, 1 mM EDTA, 1% deoxycholate] and three times with TE buffer [100 mM Tris-Cl (pH 8.0), 1 mM EDTA]. The washed beads were resuspended with 500 µl fresh elution buffer (1.0% SDS and 0.1 M sodium bicarbonate)

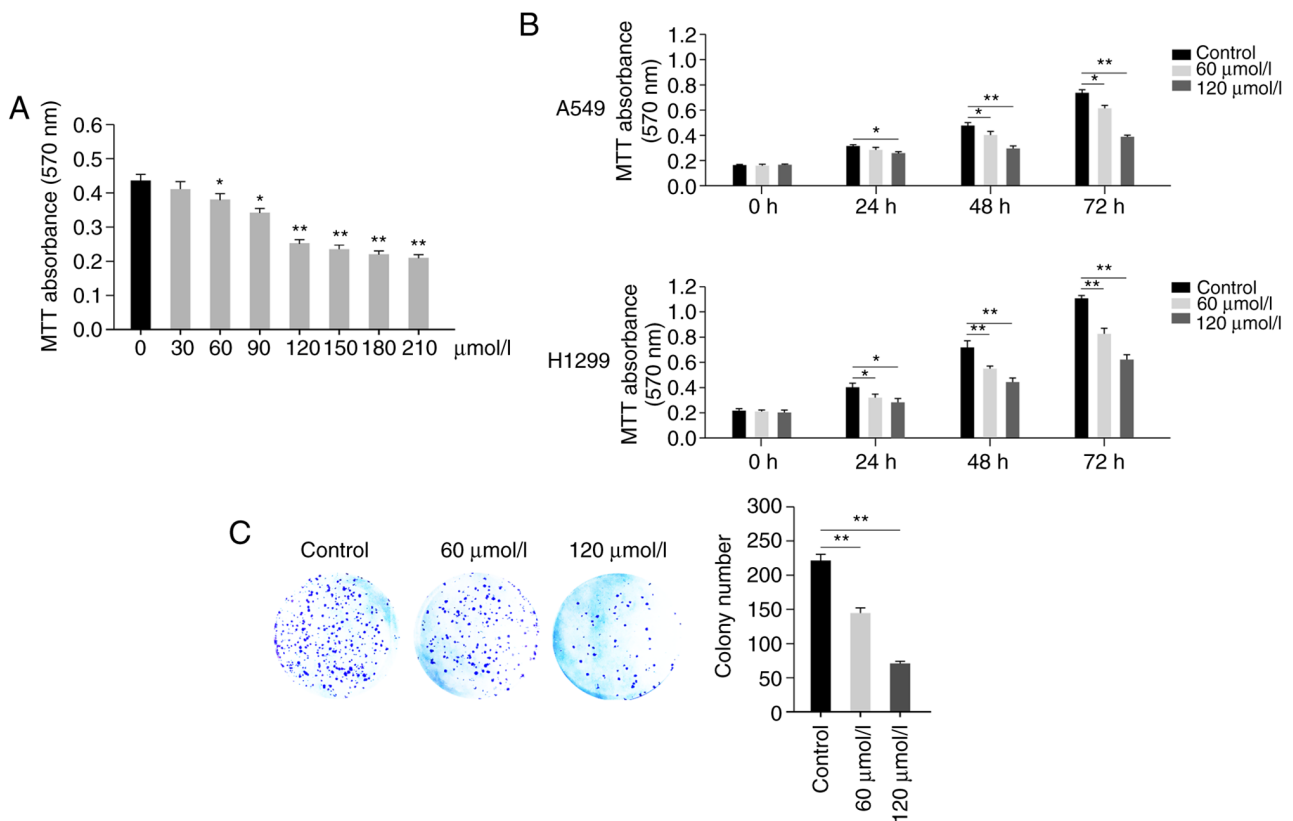


Figure 1. Propofol inhibits proliferation of human A549 cells. (A) Propofol inhibits proliferation of A549 cells in a dose-dependent manner. Viability of A549 cells was detected by MTT assay at 72 h after treatment with propofol (0, 30, 60, 90, 120, 150, 180 and 210 $\mu\text{mol/l}$). (B) Propofol inhibits proliferation of A549 and H1299 cells in a time-dependent manner. The viability of A549 or H1299 cells was detected by MTT assay at different time points (0, 24, 48 and 72 h) following treatment with propofol (60 or 120 $\mu\text{mol/l}$). The 0 h time point was 6 h after cells were seeded. (C) Propofol inhibits the colony formation of A549 cells. A total of 1,000 A549 cells were seeded into 6-well plates and treated with propofol for 7 days. Plates were fixed, stained and colony numbers were counted and calculated. Scale bar, 1 cm. Data are expressed as the mean \pm SD and analyzed using one-way ANOVA with Tukey's post hoc test. * $P < 0.05$, ** $P < 0.01$.

and incubated at 65°C for 30 min. Eluted DNA was adjusted to 300 mM NaCl and incubated at 65°C for 4 h, followed by incubation at 55°C for 1 h with 50 μg proteinase K. DNA was purified using the phenol-chloroform method and subjected to the same qPCR analysis as aforementioned (26). Primer sequences are presented in Table II.

Statistical analysis. Data are presented as the mean \pm SD of ≥ 3 independent repeats. One-way ANOVA was performed with Tukey's post hoc multiple comparisons test using GraphPad Prism software version 5.0 (GraphPad Software, Inc.). $P < 0.05$ and $P < 0.01$ were considered to indicate a statistically significant difference.

Results

Propofol inhibits proliferation of human A549 cells. In order to detect the effect of propofol on human non-small cell lung cancer, A549 cells were treated in the presence or absence of propofol (0, 30, 60, 90, 120, 150, 180 and 210 $\mu\text{mol/l}$). MTT assay indicated that propofol inhibited proliferation of A549 cells in a dose-dependent manner (Fig. 1A). Propofol exhibited significant cell proliferation inhibition at 60, 90 and 120 $\mu\text{mol/l}$ (Fig. 1A). Propofol at >120 $\mu\text{mol/l}$ resulted in little further inhibition; therefore, concentrations of 60 and 120 $\mu\text{mol/l}$ were

selected for use in further experiments (Fig. 1A). Then, the viability of A549 and H1299 cells was detected at different time points (0, 24, 48 and 72 h) following treatment in the presence or absence of propofol (60 or 120 $\mu\text{mol/l}$), which demonstrated that propofol exhibited an inhibitory effect in a time-dependent manner (Fig. 1B). Furthermore, a colony formation assay was performed; decreased colony numbers were observed in propofol-treated groups compared with the control group (Fig. 1C). These results demonstrated that propofol inhibited proliferation of A549 cells.

Propofol promotes demethylation of HACE1 gene promoter in human A549 cells. Propofol increased protein expression levels of HACE1 (Fig. 2A); further study indicated that propofol increased the expression levels of HACE1 primarily at the transcriptional, but not translational, level (Fig. 2B and C). Subsequently, a DNA methylation detection experiment was performed, which demonstrated that propofol promoted demethylation of HACE1 gene promoter in a dose-dependent manner in A549 cells (Fig. 2D).

Propofol activates HACE1-OPTN axis-mediated autophagy in human A549 and H1299 cells. Ubiquitination of the autophagy receptor OPTN by HACE1 has previously been shown to activate selective autophagy, resulting in tumor

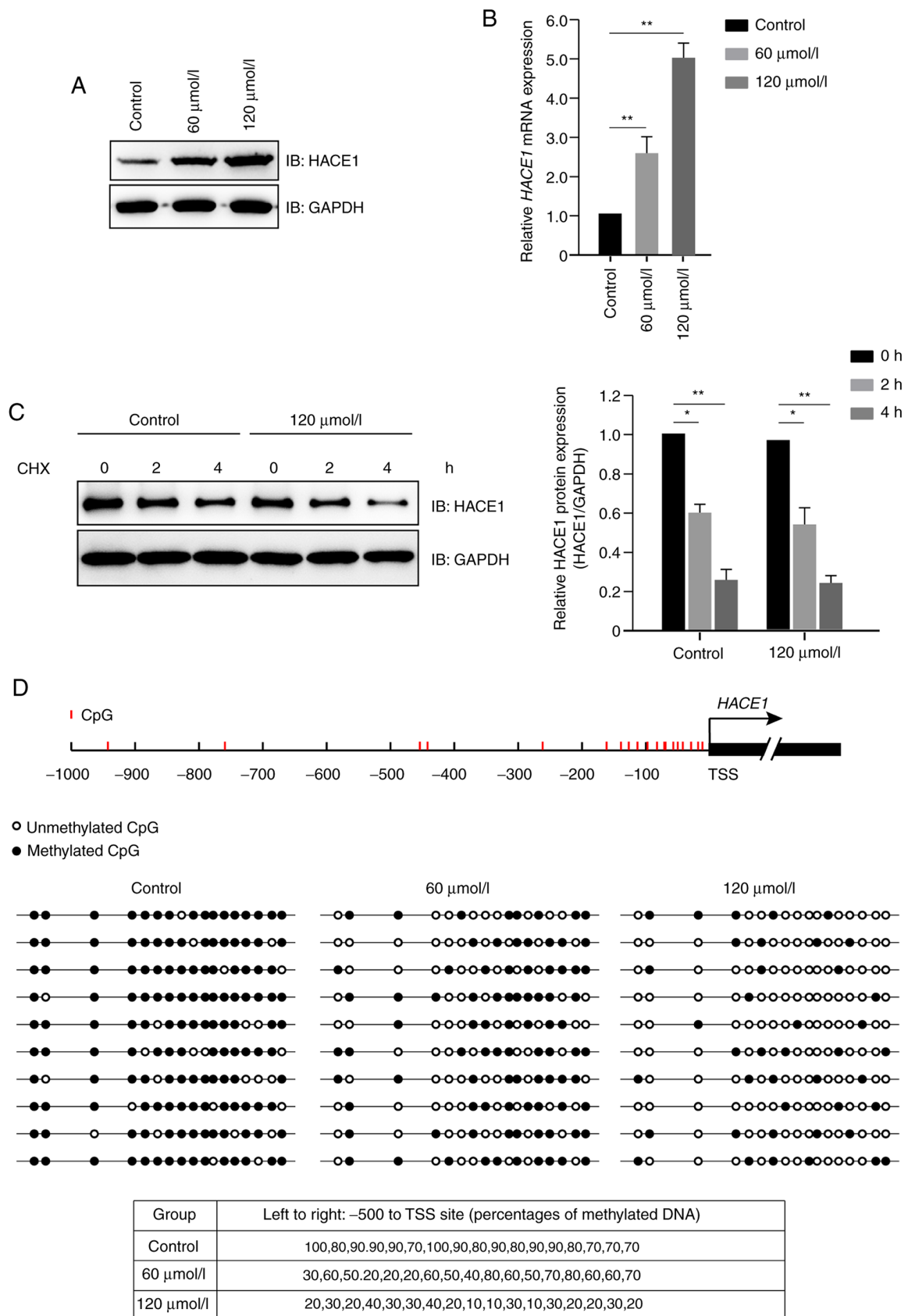


Figure 2. Propofol promotes demethylation of *HACE1* gene promoter in human A549 cells. Propofol promotes (A) protein and (B) mRNA expression levels of *HACE1*. A549 cells were treated with propofol (60 or 120 $\mu\text{mol/l}$) for 72 h, and then the protein and mRNA expression levels of *HACE1* were detected by immunoblotting and quantitative PCR, respectively. (C) Propofol does not affect the expression levels of *HACE1* on a translational level. A549 cells were treated in the presence or absence of propofol and CHX (100 $\mu\text{g/ml}$) for the indicated time duration (0, 2 or 4 h), and protein expression levels of *HACE1* were detected by immunoblotting. (D) Percentages of methylated DNA at each site in the *HACE1* gene promoter (-500 bp to TSS) were determined via bisulfite sequencing. Genomic DNA was extracted from propofol-treated A549 cells and subjected to bisulfite sequencing. Lines represent individual clones; circles represent individual CpG islands. Tables show percentage of methylated CpG for each CpG island. Data are expressed as the mean \pm SD. * $P < 0.05$, ** $P < 0.01$. *HACE1*, HECT domain and ankyrin repeat containing E3 ubiquitin protein ligase 1; CHX, cycloheximide; TSS, transcription start site; IB, immunoblot.

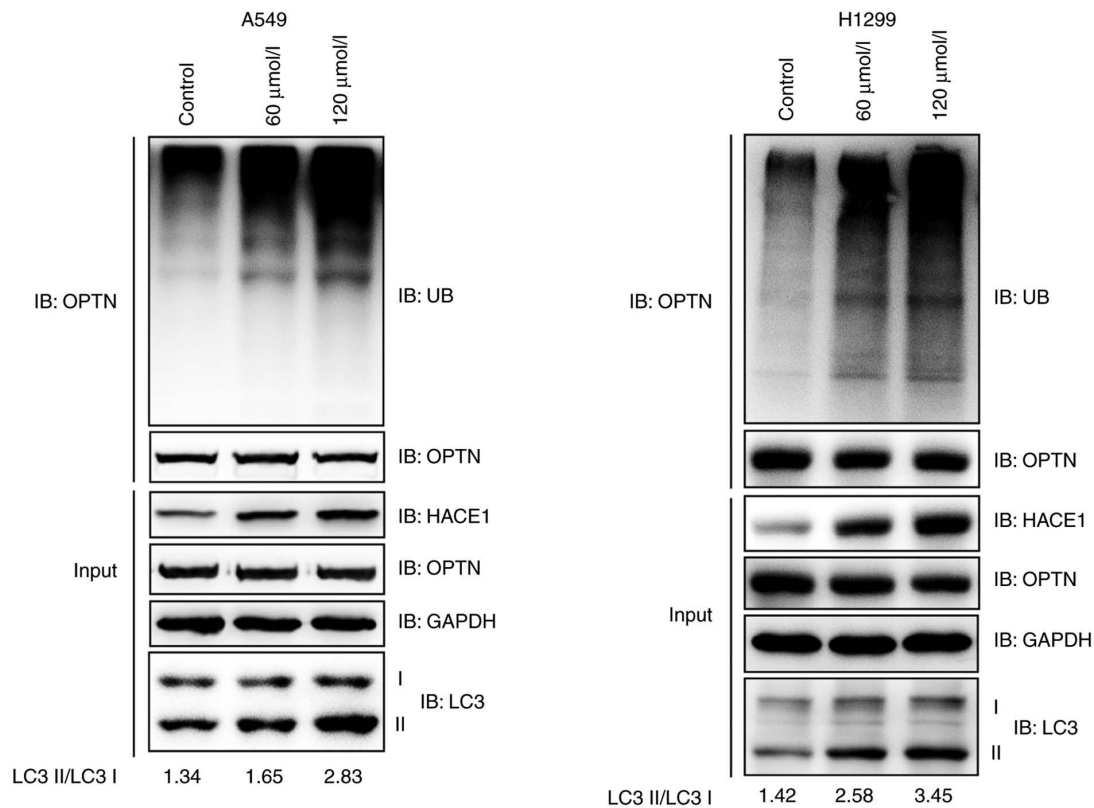


Figure 3. Propofol promotes OPTN ubiquitination and autophagy activity in human A549 and H1299 cells. A549 or H1299 cells were treated with propofol (60 or 120 $\mu\text{mol/l}$) for 72 h. Then, cell lysates were immunoprecipitated with anti-OPTN antibody and subjected to immunoblotting. LC3 II/I expression levels were also detected and calculated. OPTN, optineurin; HACE1, HECT domain and ankyrin repeat containing E3 ubiquitin protein ligase 1; IB, immunoblot; LC3, Microtubule-associated protein 1A/1B-light chain 3.

suppression in lung cancer (18). It was therefore investigated whether propofol activated HACE1-OPTN axis-mediated autophagy. The ubiquitination of OPTN notably increased when A549 or H1299 cells were treated with propofol (Fig. 3A). LC3 is the most commonly used marker of autophagosomes (18); the ratio of LC3 II to LC3 I notably increased in propofol-treated groups compared with the control group (Fig. 3A). These data indicated that propofol activated HACE1-OPTN axis-mediated autophagy.

Propofol promotes expression levels of MBD3 and binding to HACE1 gene promoter. As propofol promoted demethylation of *HACE1* gene promoter (Fig. 2C), the underlying molecular mechanism was investigated. Demethylation-associated molecules, including TET1, TET2, TET3, MBD3 and MTA2, were detected by immunoblotting in A549 cells treated in the presence or absence of propofol. Propofol exhibited no notable effect on the protein expression levels of TET1, TET2, TET2 and MTA2, but significantly increased MBD3 protein expression levels compared with the control group (Figs. 4A and S1). Further study demonstrated that propofol increased the expression levels of MBD3 primarily at the transcriptional level (Fig. 4B). As MBD3 is a transcription factor, it was then determined whether MBD3 could bind to the promoter of *HACE1*. The present study demonstrated that MBD3 preferentially bound the -1000 to -1 bp region of *HACE1* promoter (Fig. 4C) in a dose-dependent manner (Fig. 4D). These data indicated that propofol promoted demethylation of *HACE1*

promoter by regulating MBD3 expression levels and binding to *HACE1* promoter.

Propofol inhibits proliferation of human A549 cells in a MBD3-dependent manner. A total of three shRNAs for MBD3 were designed and transfected into A549 cells; immunoblotting analysis indicated that both the protein and mRNA expression levels of MBD3 were significantly decreased in cells transfected with shMBD3-1 or shMBD3-2 compared with cells transfected with scramble (Fig. 5A and B). The shRNAs for MBD3 (shMBD3-1 and sh shMBD3-2) were selected for further study. The present results also indicated that MBD3 knockdown decreased the protein expression levels of HACE1 (Fig. 5A). Furthermore, MTT and colony formation assays indicated that MBD3 knockdown abolished propofol-mediated inhibition of cell proliferation (Fig. 5C and D). These results demonstrated that propofol inhibited proliferation of human A549 cells in a MBD3-dependent manner.

Downregulation of HACE1 promotes proliferation of A549 cells. In order to investigate the effect of HACE1 on cell proliferation, two *HACE1* shRNAs were designed and tested in A549 cells. Immunoblotting analysis indicated that HACE1 significantly decreased in cells transfected with shHACE1-1 or shHACE1-2 compared with cells transfected with scramble (Fig. 5E). MTT assay demonstrated that HACE1 knockdown promoted proliferation of A549 cells (Fig. 5F).

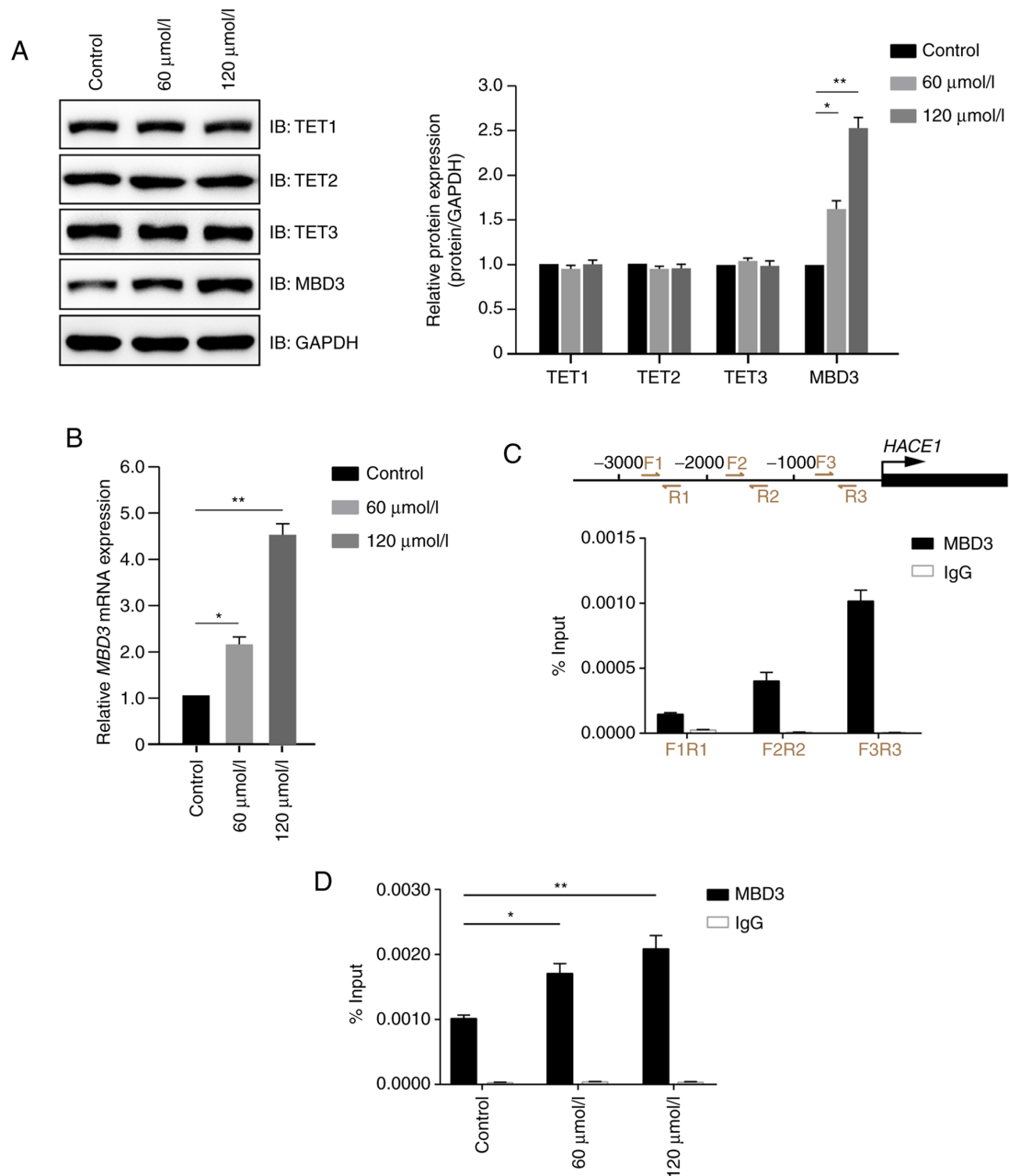


Figure 4. Propofol promotes expression levels of MBD3 and binding to *HACE1* gene promoter. A549 cells were treated with propofol for 72 h. (A) Protein expression levels of demethylation-associated molecules (TET1, TET2, TET3 and MBD3) were detected by immunoblotting. (B) Propofol promotes the mRNA expression levels of *MBD3*. mRNA expression levels of *MBD3* gene were detected by qPCR. (C) MBD3 preferentially bound to the -1,000 to -1 bp region of human *HACE1* gene promoter. Primers for different regions of *HACE1* gene promoter were designed and chromatin immunoprecipitation-quantitative PCR was performed using anti-MBD3 antibody. (D) Propofol promotes the binding of MBD3 on *HACE1* gene promoter. Data are expressed as the mean \pm SD and analyzed using one-way ANOVA with Tukey's post hoc test. * $P < 0.05$, ** $P < 0.01$. MBD3, methyl-CpG binding domain protein 3; HACE1, HECT domain and ankyrin repeat containing E3 ubiquitin protein ligase 1; TET, tet methylcytosine dioxygenase; IB, immunoblot.

Discussion

Besides anesthetic properties, propofol possesses numerous non-anesthetic effects (6). For example, Hsing *et al* (27) showed propofol decreases reactive oxygen species generation, thus inhibiting endotoxic inflammation. Cui *et al* (28) demonstrated that propofol prevents oxygen or glucose deprivation-induced autophagy in PC-12 cells, as well as cerebral ischemia-reperfusion injury in rats. The association between propofol and tumors has been extensively studied, revealing that propofol serves as a tumor suppressor or

promoting factor depend on the type of cancer (29,30). The present study demonstrated that propofol inhibited proliferation of human A549 and H1299 cells. Propofol has been shown to suppress growth, migration and invasion of A549 cells by upregulation of miR-1284 and downregulation of miR-372 (14,31), which is consistent with the results of present study. In the present study, propofol $>120 \mu\text{mol/l}$ exhibited little inhibition; however, the specific underlying mechanism requires further investigation, although it was hypothesized that the concentration of propofol reached saturation at $120 \mu\text{mol/l}$.

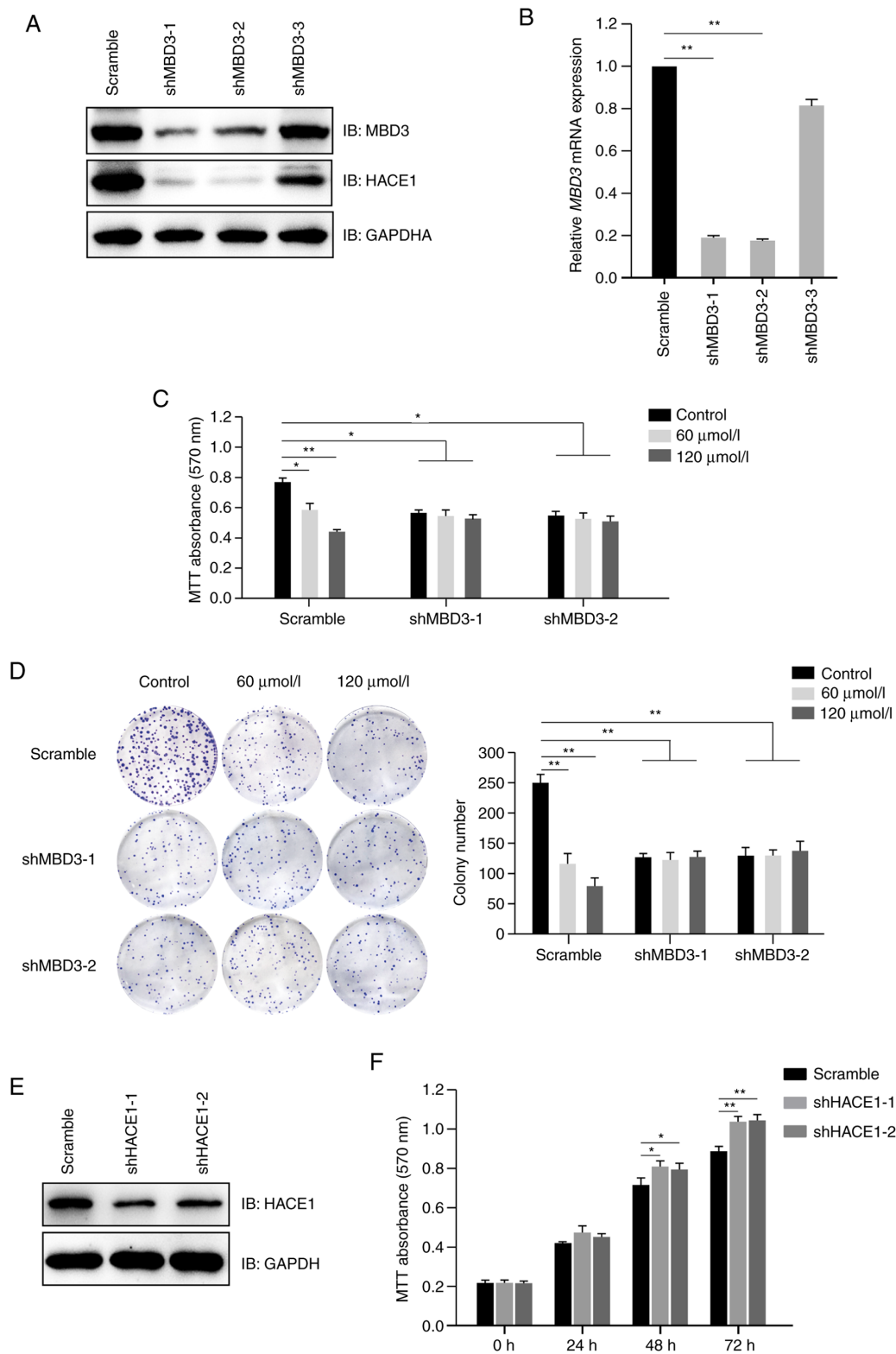


Figure 5. Propofol inhibits proliferation of human A549 cells in a MBD3-dependent manner. (A) MBD3 knockdown decreased the expression levels of HACE1. A549 cells were transfected with shRNAs (scramble control, 1, 2 or 3) for MBD3, and then subjected to screening for puromycin resistance to establish stably expressed cell lines. Protein expression levels of MBD3 and HACE1 were detected by immunoblotting. (B) Assessment of knockdown efficiency of MBD3 shRNAs by RT-qPCR. Total RNA was extracted from A549 cells stably transfected with MBD3 shRNAs, then complementary DNA was synthesized, and mRNA expression levels of *MBD3* were detected by qPCR. A549 cells stably transfected with MBD3 shRNAs (scramble, 1 or 2) were treated in the presence or absence of propofol. (C) MBD3 knockdown abolished the inhibitory effect of propofol on cell proliferation, as detected by MTT assay. (D) MBD3 knockdown abolished the inhibitory effect of propofol on cell colony formation. The viability of A549 cells was detected by MTT assay. Scale bar, 1 cm. (E) Assessment of knockdown efficiency of shRNAs for HACE1 by immunoblotting. A549 cells were transfected with shRNAs (scramble, 1 or 2) for HACE1, and then subjected to screening for puromycin resistance to establish stably expressed cell lines. The protein expression levels of HACE1 were detected by immunoblotting. (F) HACE1 knockdown promotes proliferation of A549 cells. The viability of A549 cells stably transfected with HACE1 shRNAs were detected by MTT assay. Data are expressed as the mean \pm SD of three independent experiments and analyzed using one-way ANOVA with Tukey's post hoc test. * $P < 0.05$, ** $P < 0.01$. MBD3, methyl-CpG binding domain protein 3; HACE1, HECT domain and ankyrin repeat containing E3 ubiquitin protein ligase 1; sh, short hairpin; RT-q, reverse transcription-quantitative; IB, immunoblot.

HACE1 is frequently downregulated or lost in numerous types of tumor, such as lung and liver cancer, and acts as a tumor suppressor by ubiquitinating OPTN and activating selective autophagy (18,24). The study found that propofol promoted HACE1 expression levels by demethylating *HACE1* gene promoter, which activated HACE1-OPTN axis-mediated autophagy.

In mammalian cells, DNA methylation and demethylation are critical for regulating gene expression levels and serve important roles in physiological and pathological processes, such as mammalian puberty and cancer development (32). MBD3 induces gDNA demethylation at specific targets and is also involved in maintaining the demethylated and active state of numerous genes, including progonadoliberein-1, serine/threonine-protein kinase Chk2 and 39S ribosomal protein L32, mitochondrial (26,33-35). The present findings indicated that propofol promoted expression levels of MBD3 and enhanced its binding to the *HACE1* gene promoter. This may be due to low antibody titer or weak binding of MBD3 to DNA. Further investigation is required to determine whether MBD3 promotes demethylation of *HACE1* promoter or maintains the demethylated state. The effect of propofol on mRNA expression levels of MBD3 and its specific underlying mechanism also requires further study. The present study hypothesized that propofol affects mRNA expression levels of MBD3 either by demethylating *MBD3* gene promoter or by regulating transcription of MBD3.

Selective autophagy is involved in removal of damaged or superfluous organelles from the cytosol, which is necessary to maintain homeostasis and cell function (36-39). In the present study, propofol activated selective autophagy of A549 and H1299 cells by increasing HACE1 expression levels, indicating that propofol may be a powerful therapeutic drug for lung cancer; this remains to be assessed in an animal model.

Acknowledgements

Not applicable.

Funding

The present study was supported by research grants from Science and Technology Department of Yunnan Province, and Kunming Medical University Joint Special Project [grant nos. 2018FE001-(070) and 2019FE001-(248)].

Availability of data and materials

All data generated or analyzed during this study are included in this published article.

Authors' contributions

ZW and SL conceived and designed the experiments. SL, HY, MZ, LG, YW, ZL and YQ performed the experiments, collected the data and analyzed the results. ZW and SL wrote the paper. All authors read and approved the final manuscript.

Ethics approval and consent to participate

Not applicable.

Patient consent for publication

Not applicable.

Competing interests

The authors declare that they have no competing interests.

References

- Kodama M, Higuchi H, Ishii-Maruhama M, Nakano M, Honda-Wakasugi Y, Maeda S and Miyawaki T: Multi-drug therapy for epilepsy influenced bispectral index after a bolus propofol administration without affecting propofol's pharmacokinetics: A prospective cohort study. *Sci Rep* 10: 1578, 2020.
- Sona Khan M, Trenet W, Xing N, Sibley B, Abbas M, Al-Rashida M, Rauf K and Mandiyam CD: A novel sulfonamide, 4-FS, reduces ethanol drinking and physical withdrawal associated with ethanol dependence. *Int J Mol Sci* 21: 4411, 2020.
- Yoon HK, Jun K, Park SK, Ji SH, Jang YE, Yoo S, Kim JT and Kim WH: Anesthetic agents and cardiovascular outcomes of noncardiac surgery after coronary stent insertion. *J Clin Med* 9: 429, 2020.
- Kang Y, Saito M and Toyoda H: Molecular and regulatory mechanisms of desensitization and resensitization of GABAA receptors with a special reference to propofol/barbiturate. *Int J Mol Sci* 21: 563, 2020.
- Cho YJ, Nam K, Kim TK, Choi SW, Kim SJ, Hausenloy DJ and Jeon Y: Sevoflurane, propofol and carvedilol block myocardial protection by limb remote ischemic preconditioning. *Int J Mol Sci* 20: 269, 2019.
- Sun H and Gao D: Propofol suppresses growth, migration and invasion of A549 cells by down-regulation of miR-372. *BMC Cancer* 18: 1252, 2018.
- Vasileiou I, Xanthos T, Koudouna E, Perrea D, Klonaris C, Katsargyris A and Papadimitriou L: Propofol: A review of its non-anaesthetic effects. *Eur J Pharmacol* 605: 1-8, 2009.
- Bode AM, Dong Z and Wang H: Cancer prevention and control: Alarming challenges in China. *Natl Sci Rev* 3: 117-127, 2016.
- Xia T, Zhu Y, Mu L, Zhang ZF and Liu S: Pulmonary diseases induced by ambient ultrafine and engineered nanoparticles in twenty-first century. *Natl Sci Rev* 3: 416-429, 2016.
- Zanoaga O, Braicu C, Jurj A, Rusu A, Buiga R and Berindan-Neagoe I: Progress in research on the role of flavonoids in lung cancer. *Int J Mol Sci* 20: 4291, 2019.
- Loong HH, Kwan SS, Mok TS and Lau YM: Therapeutic strategies in EGFR mutant non-small cell lung cancer. *Curr Treat Options Oncol* 19: 58, 2018.
- Xue J, Yang J, Luo M, Cho WC and Liu X: MicroRNA-targeted therapeutics for lung cancer treatment. *Expert Opin Drug Discov* 12: 141-157, 2017.
- Salne V, Huter S, Braunmueller S, Rakob L, Jacobi N, Kitzwögerer M, Wiesner C, Obrist P and Seeboeck R: Promoter methylation of selected genes in non-small-cell lung cancer patients and cell lines. *Int J Mol Sci* 21: 4595, 2020.
- Wang Q, Liu S, Zhao X, Wang Y, Tian D and Jiang W: MiR-372-3p promotes cell growth and metastasis by targeting FGF9 in lung squamous cell carcinoma. *Cancer Med* 6: 1323-1330, 2017.
- Wang X, Li W, Zhang N, Zheng X and Jing Z: Opportunities and challenges of co-targeting epidermal growth factor receptor and autophagy signaling in non-small cell lung cancer. *Oncol Lett* 18: 499-506, 2019.
- Wang H, Peng X, Huang Y, Xiao Y, Wang Z and Zhan L: Propofol attenuates hypoxia/reoxygenation-induced apoptosis and autophagy in HK-2 cells by inhibiting JNK activation. *Yonsei Med J* 60: 1195-1202, 2019.
- Xue Y, Han H, Wu L, Pan B, Dong B, Yin CC, Tian Z, Liu X, Yang Y, Zhang H, et al: iASPP facilitates tumor growth by promoting mTOR-dependent autophagy in human non-small-cell lung cancer. *Cell Death Dis* 8: e3150, 2017.
- Liu Z, Chen P, Gao H, Gu Y, Yang J, Peng H, Xu X, Wang H, Yang M, Liu X, et al: Ubiquitylation of autophagy receptor optineurin by HACE1 activates selective autophagy for tumor suppression. *Cancer Cell* 26: 106-120, 2014.

19. Liao SX, Sun PP, Gu YH, Rao XM, Zhang LY and Ou-Yang Y: Autophagy and pulmonary disease. *Ther Adv Respir Dis* 13: 1753466619890538, 2019.
20. Xu YB, Du QH, Zhang MY, Yun P and He CY: Propofol suppresses proliferation, invasion and angiogenesis by down-regulating ERK-VEGF/MMP-9 signaling in Eca-109 esophageal squamous cell carcinoma cells. *Eur Rev Med Pharmacol Sci* 17: 2486-2494, 2013.
21. Xu X, Li C, Gao X, Xia K, Guo H, Li Y, Hao Z, Zhang L, Gao D, Xu C, *et al*: Excessive UBE3A dosage impairs retinoic acid signaling and synaptic plasticity in autism spectrum disorders. *Cell Res* 28: 48-68, 2018.
22. Li C, Han T, Guo R, Chen P, Peng C, Prag G and Hu R: An integrative synthetic biology approach to interrogating cellular ubiquitin and ufm signaling. *Int J Mol Sci* 21: 4231, 2020.
23. Longchamps RJ, Castellani CA, Yang SY, Newcomb CE, Sumpter JA, Lane J, Grove ML, Guallar E, Pankratz N, Taylor KD, *et al*: Evaluation of mitochondrial DNA copy number estimation techniques. *PLoS One* 15: e0228166, 2020.
24. Yu Z, Li Y, Han T and Liu Z: Demethylation of the HACE1 gene promoter inhibits the proliferation of human liver cancer cells. *Oncol Lett* 17: 4361-4368, 2019.
25. Li H, Liang Z, Yang J, Wang D, Wang H, Zhu M, Geng B and Xu EY: DAZL is a master translational regulator of murine spermatogenesis. *Natl Sci Rev* 6: 455-468, 2019.
26. Li C, Lu W, Yang L, Li Z, Zhou X, Guo R, Wang J, Wu Z, Dong Z, Ning G, *et al*: MKRN3 regulates the epigenetic switch of mammalian puberty via ubiquitination of MBD3. *Natl Sci Rev* 7: 671-685, 2020.
27. Hsing CH, Lin MC, Choi PC, Huang WC, Kai JI, Tsai CC, Cheng YL, Hsieh CY, Wang CY, Chang YP, *et al*: Anesthetic propofol reduces endotoxic inflammation by inhibiting reactive oxygen species-regulated Akt/IKK β /NF- κ B signaling. *PLoS One* 6: e17598, 2011.
28. Cui D, Wang L, Qi A, Zhou Q, Zhang X and Jiang W: Propofol prevents autophagic cell death following oxygen and glucose deprivation in PC12 cells and cerebral ischemia-reperfusion injury in rats. *PLoS One* 7: e35324, 2012.
29. Zhang L, Wang N, Zhou S, Ye W, Jing G and Zhang M: Propofol induces proliferation and invasion of gallbladder cancer cells through activation of Nrf2. *J Exp Clin Cancer Res* 31: 66, 2012.
30. Du Q, Liu J, Zhang X, Zhang X, Zhu H, Wei M and Wang S: Propofol inhibits proliferation, migration, and invasion but promotes apoptosis by regulation of Sox4 in endometrial cancer cells. *Braz J Med Biol Res* 51: e6803, 2018.
31. Liu WZ and Liu N: Propofol inhibits lung cancer A549 cell growth and epithelial-mesenchymal transition process by upregulation of MicroRNA-1284. *Oncol Res* 27: 1-8, 2018.
32. Xu X, Tao Y, Gao X, Zhang L, Li X, Zou W, Ruan K, Wang F, Xu GL and Hu R: A CRISPR-based approach for targeted DNA demethylation. *Cell Discov* 2: 16009, 2016.
33. Brown SE, Suderman MJ, Hallett M and Szyf M: DNA demethylation induced by the methyl-CpG-binding domain protein MBD3. *Gene* 420: 99-106, 2008.
34. Peng L, Li Y, Xi Y, Li W, Li J, Lv R, Zhang L, Zou Q, Dong S, Luo H, *et al*: MBD3L2 promotes Tet2 enzymatic activity for mediating 5-methylcytosine oxidation. *J Cell Sci* 129: 1059-1071, 2016.
35. Brown SE and Szyf M: Epigenetic programming of the rRNA promoter by MBD3. *Mol Cell Biol* 27: 4938-4952, 2007.
36. Lee CW, Wilfling F, Ronchi P, Allegretti M, Mosalaganti S, Jentsch S, Beck M and Pfander B: Selective autophagy degrades nuclear pore complexes. *Nat Cell Biol* 22: 159-166, 2020.
37. Yamasaki A, Alam JM, Noshiro D, Hirata E, Fujioka Y, Suzuki K, Ohsumi Y and Noda NN: Liquidity is a critical determinant for selective autophagy of protein condensates. *Mol Cell* 77: 1163-1175.e9, 2020.
38. Zhao ZQ, Yu ZY, Li J and Ouyang XN: Gefitinib induces lung cancer cell autophagy and apoptosis via blockade of the PI3K/AKT/mTOR pathway. *Oncol Lett* 12: 63-68, 2016.
39. Ren S, Ding C and Sun Y: Morphology remodeling and selective autophagy of intracellular organelles during viral infections. *Int J Mol Sci* 21: 3689, 2020.



This work is licensed under a Creative Commons Attribution-NonCommercial-NoDerivatives 4.0 International (CC BY-NC-ND 4.0) License.